Progress of Theoretical Physics, Vol. 81, No. 5, May 1989

Theory of Surface-Induced Magnetism in Adsorbed ^{3}He Films. II

——*Curie-Weiss Temperature (Reinvestigated), Curie Constant and Liquid-Layer Susceptibility*——

Shuichi TASAKI

Department of Physics, Kyoto University, Kyoto 606

(Received October 28, 1988; Revised February 27, 1989)

Within a three-layer model, previously proposed by the author, the Curie-Weiss temperature of adsorbed ^{3}He films is reinvestigated by taking all exchange constants into account, and the Curie constant and liquid-layer susceptibility are calculated. Better agreement with the experiment by Franco et al. is obtained for the coverage-dependence of the Curie-Weiss temperature. It is also found that 1) the Curie constant is almost independent of the density of liquid-layer atoms and 2) the susceptibility of two liquid layers is negligible at low temperatures compared with that of the solid layer.

§ 1. Introduction

Ferromagnetism of adsorbed ^{3}He layers has attracted considerable attention[1),2)] since its first discovery in ^{3}He on Mylar sheets. Recently Franco, Rapp and Godfrin[3)] have measured a Curie-Weiss temperature as a function of the number of adsorbed layers. In a previous paper[4)] (hereafter referred to as I), using a three-layer lattice model (schematically shown in Fig. 1), we have derived an effective spin Hamiltonian for the solid-layer atoms

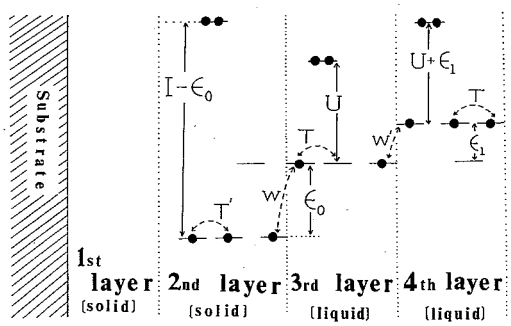

Fig. 1. Schematic representation of the interface model. Site levels are represented by small segments, ^{3}He atoms by solid circles and transfer energies by broken segments. $T(T')$ is the strength of hopping in the liquid (solid) layers, $w(w')$, strength of transfer between the second and third (the third and fourth) layers, $U(I)$, the strength of ^{3}He-^{3}He interaction in the liquid (solid) layers, and $-\varepsilon_0(\varepsilon_1)$, the site energy of the second (fourth) layer measured from that of the third layer. For their values, see the text.

$$H^{\mathrm{eff}}=-\frac{1}{\hbar^2}\sum_{i,j}J_{ij}\boldsymbol{S}_i\cdot\boldsymbol{S}_j \qquad (1\cdot1)$$

and tried to explain the results of Ref. 3). Although the nearest-neighbor exchange terms alone have been taken into account there, as is well known and shown in Fig. 2, the exchange constant J_{ij} strongly depends on the relative position $\boldsymbol{R}_{ij}$. Therefore we must also consider exchange constants other than the nearest-neighbor one and reinvestigate the Curie-Weiss temperature.

In our model, the observed surface-induced ferromagnetism is explained in terms of the indirect spin exchange. The Curie constant as well as the Curie-Weiss temperature depends on the liquid-layer density, and the effect of the liquid layers cannot be disregarded.

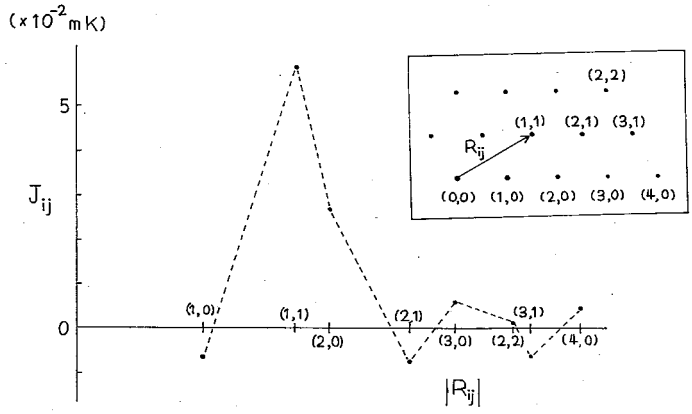

Fig. 2. The exchange constant J_{ij} vs the relative position $\boldsymbol{R}_{ij}$ when 97% of the third layer is filled ($n=0.97$ and $\bar{n}=1.84$). The horizontal axis is the magnitude of $\boldsymbol{R}_{ij}$ and an integer pair denotes a site index. The assignment of an index to a lattice site is shown in the inset.

Therefore we must check whether the density-dependence of the Curie constant and the ratio of the liquid-layer susceptibility to the solid-layer one are consistent with the experiments.

The purpose of this paper is to reinvestigate the Curie-Weiss temperature and to investigate the Curie constant and the liquid-layer susceptibility. The remaining part of this paper is arranged as follows: In § 2, the Curie-Weiss temperature will be reinvestigated. In § 3, the Curie constant and the liquid-layer susceptibility will be studied. Section 4 is devoted to a summary. In Appendix A, a formal theory of an effective Hamiltonian will be given and Eq. (3·5) will be derived. In Appendix B, the ground-state properties of the liquid layers are shown.

§ 2. The Curie-Weiss temperature

As pointed out in the Introduction, to estimate the Curie-Weiss temperature, we must consider exchange constants other than the nearest-neighbor one. Since the exchange constant J_{ij} decreases for large $|\boldsymbol{R}_{ij}|$ as $\{\sin(2k_f|\boldsymbol{R}_{ij}|+\varphi)\}/|\boldsymbol{R}_{ij}|^2$ the mean-field Curie-Weiss temperature

$$T_c=\frac{1}{2}\sum_{j(\neq i)}J_{ij} \tag{2·1}$$

is a good approximation except the case where the liquid-layer Fermi energy is placed near the band edges.

With the aid of Eqs. (5·13b) ~ (5·14) of I, we have

$$T_c=T_c^H+T_c^{R1}+T_c^{R2}+T_c^{R3}, \tag{2·2a}$$

where T_c^H is Héritier's contribution

$$T_c^H=3J_{ij}^H, \qquad ((i,j) \text{ is a nearest-neighbor pair}) \tag{2·2b}$$

T_c^{R1}, the lower-band RKKY contribution

$$T_c^{R1}=\frac{1}{2}\left(\frac{qa}{\varepsilon_0 a'}\right)^2\frac{1}{N_s}\sum_{\boldsymbol{k}}|w(\boldsymbol{k})|^4\,u_{\boldsymbol{k}}{}^{-2}\,\delta(E_{\boldsymbol{k}}{}^{-}-\mu)-\frac{1}{2}J_{ii}^{R1}\,, \tag{2·2c}$$

T_c^{R2}, the interband RKKY contribution

$$T_c^{R2}=\left(\frac{qa}{\varepsilon_0 a'}\right)^2\frac{1}{N_s}\sum_{\boldsymbol{k}}|w(\boldsymbol{k})|^4\frac{u_{\boldsymbol{k}}{}^{+}u_{\boldsymbol{k}}{}^{-}}{E_{\boldsymbol{k}}{}^{+}-E_{\boldsymbol{k}}{}^{-}}\{\theta(E_{\boldsymbol{k}}{}^{+}-\mu)-\theta(E_{\boldsymbol{k}}{}^{-}-\mu)\}-\frac{1}{2}J_{ii}^{R2} \tag{2·2d}$$

and T_c^{R3}, the upper-band RKKY contribution

$$T_c^{R3}=\frac{1}{2}\left(\frac{qa}{\varepsilon_0 a'}\right)^2\frac{1}{N_s}\sum_{\boldsymbol{k}}|w(\boldsymbol{k})|^4\,u_{\boldsymbol{k}}{}^{+2}\,\delta(E_{\boldsymbol{k}}{}^{+}-\mu)-\frac{1}{2}J_{ii}^{R3}\,. \tag{2·2e}$$

In the above, a function $\delta(x)$ stands for the delta function, μ is the chemical potential, N_s, the number of the third-layer sites, q, the inverse of the third-layer mass enhancement factor, and a and a', the lattice constants of the liquid and solid layers respectively. The upper-band (lower-band) energy $E_{\boldsymbol{k}}{}^{+}(E_{\boldsymbol{k}}{}^{-})$ is given by Eq. (5·9) in I; the upper-band (lower-band) coherence factor $u_{\boldsymbol{k}}{}^{+}(u_{\boldsymbol{k}}{}^{-})$, by Eq. (5·10) in I; and the $\boldsymbol{k}$-dependent transfer strength $w(\boldsymbol{k})$ between the second and third layers, by Eq. (6·1c) in I. Héritier's exchange constant J_{ij}^{H} is given by Eq. (5·14) in I and the lower-band contribution J_{ij}^{R1}, the interband contribution J_{ij}^{R2} and the upper-band contribution J_{ij}^{R3} to the RKKY exchange constant are given by Eqs. (5·13b)~(5·13d) in I. In Eq. (2·2) and the following, the $\boldsymbol{k}$-sums are taken over the first Brillouin zone. To compare the results with experiments, we set the primary parameters (see Fig. 1) as $a'=3.7$ Å, $a=4$ Å, $T=w'=1.4$ K, $w=1.3$ K, $T'=300$ mK, $U=22.4$ K,*)

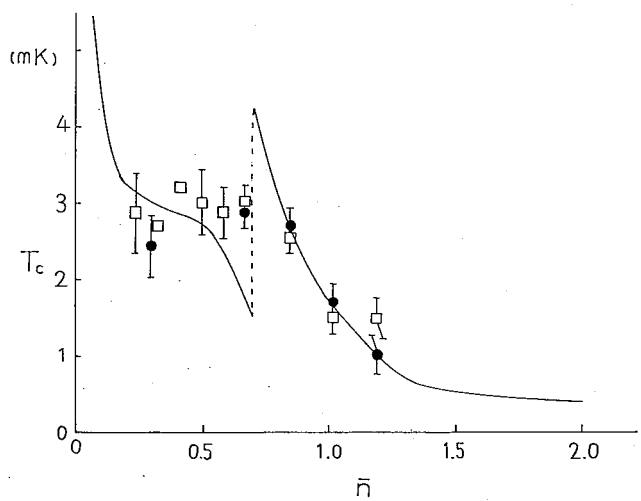

Fig. 3. The Curie-Weiss temperature T_c vs the number $\bar{n}$ of the liquid-layer atoms per site. Squares and solid circles are the results of Ref. 3).

*) The values of w, w', T′ and U used in I are inadequate since there were errors in numerical integrations (see Errata of I). The value 300 mK of T' is much larger than that in I (70 mK). But it is plausible, for the hopping in solid ^{3}He is of order of 100 mK.[5] Then the Fermi energy of order of 10 mK, which is observed experimentally, may be explained by the strong almost-localized-Fermion effect. Note that the singular behaviors of T_c do not result from the correction given here, but from the lattice sum in Eq. (2·1).

$$\varepsilon_0 = 10 + 5.6n - 4.5n' \quad \text{(K)}$$

and

$$\varepsilon_1 = 7.2 + 4.5n' - 4.6n - 4.1 \max(0, 2.1n' - 1) \quad \text{(K)},$$

where n and n' are the numbers of atoms per site in the third and fourth layers respectively. Then, when n reaches 1, T_c becomes 0.4 mK, which agrees well with the experimental value of 0.5 mK[1] of the liquid ^{3}He in the restricted geometry. The dependence of T_c on the number of liquid-layer atoms per site $\bar{n} = n + n'$ also agrees well with the results of Ref. 3) except at $\bar{n} \cong 0$ and $\bar{n} \cong 0.7$, as shown in Fig. 3. As shown in Fig. 5, the singular behaviors of T_c near $\bar{n} = 0$ and $\bar{n} = 0.7$ come from those of T_c^{R1} and T_c^{R3} respectively. Since the first terms on the right-hand sides of (2·2c) and (2·2e) are essentially the densities of states of the new bands, both singularties are caused by the well-known fact that the density of states of a two-dimensional system has a finite value at a band edge. This is, however, an artifact of our treatment: In actual systems, the values of site energies (ε_0 and ε_1) and molecular fields (L_2 and L_2' in Eq. (B·1), see Appendix B) fluctuate and act like random potentials to the liquid-layer atoms and, as a result, the densities of states as well as T_c^{R1} and T_c^{R3} become small at the band edges: The jumps in T_c are tempered in actual systems.*)

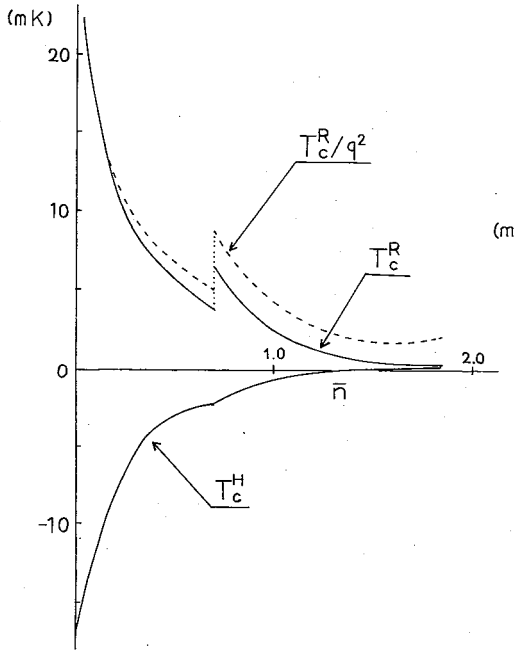

Fig. 4. The RKKY contribution T_c^R and Hēritier's contribution T_c^H to the Curie-Weiss temperature as functions of the number $\bar{n}$ of liquid-layer atoms per site. Broken line indicates T_c^R/q^2.

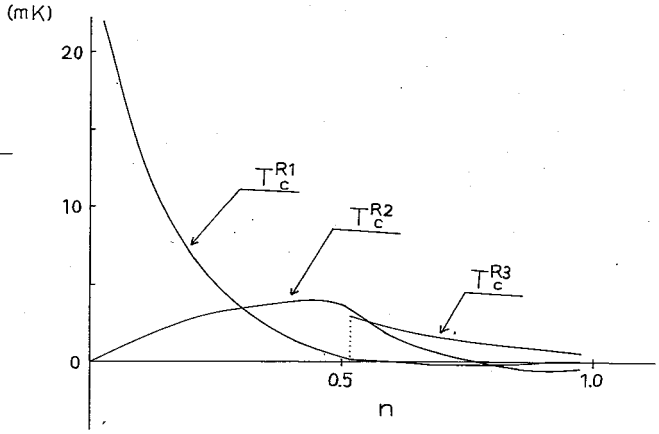

Fig. 5. Individual contributions to T_c^R as functions of the number n of the third-layer atoms per site. T_c^{R1}: the lower-band contribution, T_c^{R2}: the interband contribution and T_c^{R3}: the upper-band contribution.

*) In other words, the fluctuations reduce the range of the RKKY coupling which becomes very long when the Fermi energy is placed near the band edges.

Moreover, it is shown experimentally that the second layer, which is assumed to be solid here, is rather liquid at the vicinity of $\bar{n}=0$. This may be another reason why the singular behavior of T_c near $\bar{n}=0$ is not observed experimentally, since the number of correlating spins in the liquid state is less than that in the solid state.

Héritier's contribution T_c^H, RKKY contribution $T_c^R=T_c^{R1}+T_c^{R2}+T_c^{R3}$ and T_c^R/q^2 are shown in Fig. 4 as functions of $\bar{n}$. Appreciable decrease in T_c^R at $\bar{n}>0.7$ is caused by the presence of the factor q^2, which decreases rapidly as the third layer becomes complete. Indeed, without this factor, T_c^R does not decrease at $\bar{n}>1.5$ as shown in Fig. 4 (broken line). Physically speaking, the decrease in q or the increase in the mass of a liquid-layer atom suppresses the virtual hopping between the solid and liquid layers and also suppresses the Curie-Weiss temperature. The separate RKKY contributions T_c^{R1}, T_c^{R2} and T_c^{R3} are shown in Fig. 5 as functions of n. Note that the sum of T_c^{R2} and T_c^{R3} is always positive, while T_c^{R1} changes sign. This implies that the existence of the fourth layer, which gives T_c^{R2} and T_c^{R3}, is essential to make T_c always ferromagnetic. These results are the same as those of I. Thus, while the inadequate parameters are used, the physical conclusions of I are unchanged.

§ 3. The Curie constant

The ^{3}He-substrate interface under the magnetic field B along the z-axis is described by a Hamiltonian H which is composed of a solid-layer energy H_s, a liquid-solid interaction H_{l-s}, a liquid-layer energy H_l and Zeeman terms:

$$H=H_s+H_l+H_{l-s}-\gamma B(\sum_i \sigma_i^z+\sum_i \sigma_i'^z+\sum_i S_i^z)\,,$$

where γ is the gyromagnetic ratio of ^{3}He and S_i^z, σ_i^z and $\sigma_i'^z$ are z-components of i-site spin operators for the second, third and fourth layers.

The liquid-solid interaction H_{l-s} causes the change of the Curie constant through two processes: Liquid-layer atoms change the magnetic field felt by a solid-layer spin, and polarized solid-layer spins induce magnetic moments in the liquid layers. The former is described by a change in the Zeeman term of an effective Hamiltonian for the solid-layer spins, and the latter by the expectation value of the liquid-layer spins which is proportional to the solid-layer spins. In the following, we will investigate the two processes separately and estimate the Curie constant numerically.

3.1. *Change in Zeeman term of effective Hamiltonian*

In I, we derived an effective Hamiltonian for the solid-layer atoms. The results are also valid in the present case:

$$H_s^{\text{eff}}=H_s-\gamma B\sum_i S_i^z+\frac{1}{2}\langle\zeta_B|[S, H_{l-s}]|\zeta_B\rangle+O\left(w\left(\frac{w}{\varepsilon_0}\right)^2\right), \tag{3·1}$$

where S is the lowest order generator of the Schrieffer-Wolff transformation (Eq. (3·3) of I) and $|\zeta_B\rangle$ the ground state of the liquid-layer Hamiltonian with the Zeeman terms: $H_l-\gamma B(\sum_i\sigma_i^z+\sum_i\sigma_i'^z)$. When every solid-layer site is occupied by one atom,

Eq. (3·1) is cast into a spin Hamiltonian. When $B=0$, the lowest order correction (the third term of Eq. (3·1)) does not contribute to the spin Hamiltonian, but, when $B \neq 0$, it gives a term which is proportional to $\sum_i S_i^z$:

$$\frac{1}{2}\langle\zeta_B|[S, H_{l-s}]|\zeta_B\rangle = -\alpha\sum_i S_i^z + (c\text{-number terms}) + O\left(w\left(\frac{w}{\varepsilon_0}\right)^2\right), \tag{3·2a}$$

where

$$\alpha = \frac{i}{2\hbar}\int_0^\infty dt e^{-\eta t} e^{-i\varepsilon_0 t}\langle\zeta_B|\{\Gamma_{i\uparrow}(t)\Gamma_{i\uparrow}^+ - \Gamma_{i\downarrow}(t)\Gamma_{i\downarrow}^+\}|\zeta_B\rangle + (\text{h.c.}) \tag{3·2b}$$

with $\hbar$ the Planck constant divided by 2π. The operator $\Gamma_{i\sigma}(t)$ is given by Eq. (4·4) of I and η is an infinitesimal positive constant.

When B is small, α is well approximated by a B-linear term and gives a correction to the solid-layer Zeeman term:

$$-\gamma B\sum_i S_i^z \longrightarrow -\gamma\left(1+\frac{\partial\alpha}{\partial(\gamma B)}\Big|_{B=0}\right)B\sum_i S_i^z .$$

The coefficient of proportion $\{\partial\alpha/\partial(\gamma B)\}|_{B=0}$ is given by

$$\frac{\partial\alpha}{\partial(\gamma B)}\Big|_{B=0} = \frac{1}{2\hbar}\sum_j\int_0^\infty dt\int_0^\infty dt' e^{-\eta t}e^{-\eta t'}e^{-i\varepsilon_0 t}\langle\zeta|A_{ij}(t, t')|\zeta\rangle + (\text{h.c.}), \tag{3·3a}$$

where

$$\begin{aligned} A_{ij}(t, t') = &\{\Gamma_{i\uparrow}(t)\Gamma_{i\uparrow}^+ - \Gamma_{i\downarrow}(t)\Gamma_{i\downarrow}^+\}\bar{p}\{\sigma_j^z(t') + \sigma_j'^z(t')\} \\ &-\{\sigma_j^z(t') + \sigma_j'^z(t')\}\bar{p}\{\Gamma_{i\uparrow}(t)\Gamma_{i\uparrow}^+ - \Gamma_{i\downarrow}(t)\Gamma_{i\downarrow}^+\} . \end{aligned} \tag{3·3b}$$

$|\zeta\rangle$ is the ground state of H_l and $\bar{p}=1-|\zeta\rangle\langle\zeta|$.

As explained in I, we estimate the correlation functions in Eq. (3·3) by the Gutzwiller approximation. Then we have

$$\frac{\partial\alpha}{\partial(\gamma B)}\Big|_{B=0} = -\frac{q}{\varepsilon_0}\frac{1}{N_s}\sum_{\boldsymbol{k}}|w(\boldsymbol{k})|^2\{u_{\boldsymbol{k}}{}^+\delta(E_{\boldsymbol{k}}{}^+ - \mu) + u_{\boldsymbol{k}}{}^-\delta(E_{\boldsymbol{k}}{}^- - \mu)\} . \tag{3·4a}$$

Note that the effect of the applied magnetic field on the exchange constants is negligible, since the effect is of higher order with respect to B than that on α.

3.2. *Liquid-layer moment induced by solid-layer spins*

In this subsection, we calculate the expectation values of the solid- and liquid-layer moments. Since the Schrieffer-Wolff transformation conserves the total spin, we have only to carry out the calculations in transformed representation.

First, we must obtain the ground state of the original Hamiltonian. By comparing the perturbation series for the original and effective Hamiltonians, we have

$$|\psi\rangle = C_N W|\phi\rangle|\zeta_B\rangle , \tag{3·5}$$

where $|\psi\rangle$ is the ground state of the original Hamiltonian; $|\phi\rangle$, that of the effective Hamiltonian for the solid-layer atoms; C_N, the normalization constant and W, the mixing operator (see Appendix A). In the lowest order in H_{l-s}, we find

$$C_N=1+O\left(\left(\frac{w}{\varepsilon_0}\right)^2\right), \tag{3·6a}$$

$$W=1+\frac{i}{2}\int_0^\infty dt\bar{p}_B[S, H_{l-s}](t)+O\left(\left(\frac{w}{\varepsilon_0}\right)^2\right), \tag{3·6b}$$

where $\bar{p}_B=1-|\zeta_B\rangle\langle\zeta_B|$ and time evolution of the operator in the integrand of Eq. (3·6b) is generated by a total Hamiltonian without H_{l-s}; $H_s+H_l-\gamma B(\sum_i\sigma_i^z+\sum_i\sigma_i'^z)$. Then, with the aid of Eqs. (3·5) and (3·6), we obtain the expectation values of the solid- and liquid-layer spins,

$$\langle\phi|\sum_i S_i^z|\psi\rangle=\langle\phi|\sum_i S_i^z|\phi\rangle+O\left(\left(\frac{w}{\varepsilon_0}\right)^2\right), \tag{3·7a}$$

$$\langle\phi|\{\sum_i\sigma_i^z+\sum_i\sigma_i'^z\}|\psi\rangle=\langle\zeta_B|\{\sum_i\sigma_i^z+\sum_i\sigma_i'^z\}|\zeta_B\rangle$$
$$+\langle\zeta_B|\Delta\sigma|\zeta_B\rangle+\beta\langle\phi|\sum_i S_i^z|\phi\rangle+O\left(\left(\frac{w}{\varepsilon_0}\right)^2\right), \tag{3·7b}$$

where

$$\Delta\sigma=\frac{1}{4}\sum_{i,j}\int_0^\infty dt\int_0^\infty dt' e^{-\eta t}e^{-\eta t'}e^{i\varepsilon_0 t}B_{ij}(t, t')+(\text{h.c.}) \tag{3·8a}$$

and

$$\beta=\frac{1}{2\hbar}\sum_j\int_0^\infty dt\int_0^\infty dt' e^{-\eta t}e^{-\eta t'}e^{i\varepsilon_0 t}\langle\zeta|C_{ij}(t, t')|\zeta\rangle+(\text{h.c.}) \tag{3·9a}$$

with

$$B_{ij}(t, t')=\sum_\sigma\Gamma_{i\sigma}(t')\Gamma_{i\sigma}^+(t+t')\bar{p}_B\{\sigma_j^z+\sigma_j'^z\}$$
$$-\{\sigma_j^z+\sigma_j'^z\}\bar{p}_B\sum_\sigma\Gamma_{i\sigma}(t')\Gamma_{i\sigma}^+(t+t') \tag{3·8b}$$

and

$$C_{ij}(t, t')=\{\Gamma_{i\uparrow}(t')\Gamma_{i\uparrow}^+(t+t')-\Gamma_{i\downarrow}(t')\Gamma_{i\downarrow}^+(t+t')\}\bar{p}\{\sigma_j^z+\sigma_j'^z\}$$
$$-\{\sigma_j^z+\sigma_j'^z\}\bar{p}\{\Gamma_{i\uparrow}(t')\Gamma_{i\uparrow}^+(t+t')-\Gamma_{i\downarrow}(t')\Gamma_{i\downarrow}^+(t+t')\}. \tag{3·9b}$$

In Eq. (3·7), only the linear terms with respect to B are retained. Time evolution of $\Gamma_{i\sigma}$ in Eq. (3·8b) is generated by $H_l-\gamma B(\sum_i\sigma_i^z+\sum_i\sigma_i'^z)$, and that in Eq. (3·9b) by H_l. Equation (3·7b) shows that the liquid-layer moment induced by the solid-layer spins is $\beta\sum_i S_i^z$.

After calculating the correlation functions in Eq. (3·9a) in the Gutzwiller approximation, we find a relation

$$\beta=\left.\frac{\partial\alpha}{\partial(\gamma B)}\right|_{B=0}. \tag{3·10}$$

Equation (3·10) shows that the liquid-solid interaction H_{l-s} changes the gyromagnetic ratio of a solid-layer atom to $(1+\beta)\gamma$. The first and second terms on the right-hand

side of Eq. (3·7b) contribute to the liquid-layer susceptibility. Note that the latter is negligible because it is smaller than the former by a factor of w/ε_0 and the former is very small compared with the solid-layer susceptibility.

3.3 *Numerical results*

As a result, the Curie constant C is given by

$$\frac{C}{C_0}=(1+\beta)^2\,, \tag{3·11}$$

where C_0 is the bare Curie constant

$$C_0=\frac{\hbar^2\gamma^2}{4}\bar{N}_s$$

with $\bar{N}_s$ the number of solid-layer atoms.

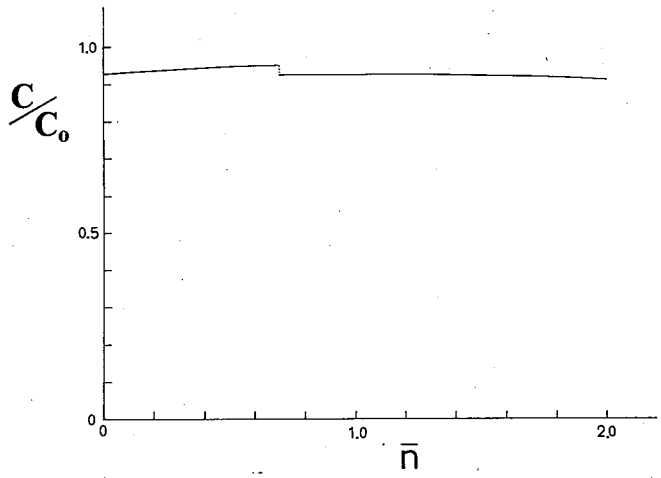

Fig. 6. The Curie constant C vs the number $\bar{n}$ of liquid-layer atoms per site. C_0 denotes the bare Curie constant.

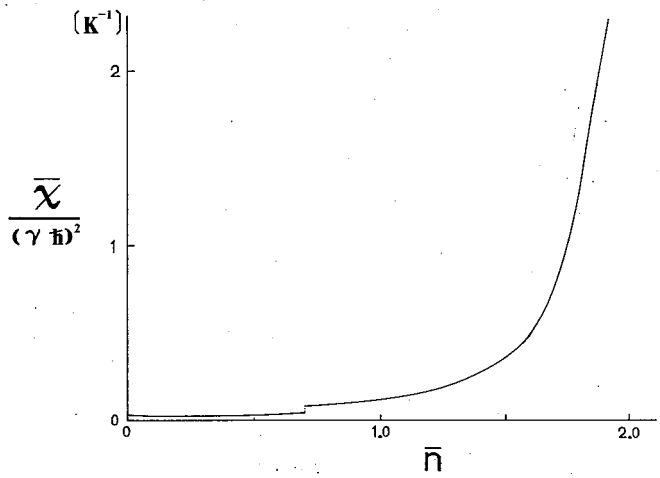

Fig. 7. Liquid-layer susceptibility $\bar{\chi}$ per solid-layer site vs the number $\bar{n}$ of liquid-layer atoms per site.

In Fig. 6, the Curie constant is shown as a function of the number $\bar{n}=n+n'$ of liquid-layer atoms per site. The abrupt decrease at $\bar{n}\cong 0$ and discontinuity at $\bar{n}\cong 0.7$ reflect the finiteness of the band-edge densities of states of the lower and upper bands respectively. From Fig. 6, the Curie constant C is found to vary within the range of $93\%\pm 2\%$ of the bare value C_0. This is consistent with the data of Ref. 3), which shows that the Curie constant is almost independent of the layer thickness. At $\bar{n}=0.56$, where the experiment of Ref. 6) was carried out, we have $C/C_0\cong 0.95$, which gives a slope $(d\chi_t^{-1}/dT_e)$ by two percent larger than that of bare spins, where χ_t is the susceptibility of the first two solid layers (see Fig. 1). The value is consistent with that of Ref. 6). Physically the reduction of the Curie constant can be explained as follows: The transfer of atoms between the liquid and solid layers induces a spin-spin coupling between liquid- and solid-layer atoms, which is antiferromagnetic like that in the Anderson model.[7] As a result, the solid-layer spins are shielded by the liquid-layer atoms and their Curie constant is reduced.

Finally we turn our attention to the liquid-layer susceptibility (for its calculation, see Appendix B). In Fig. 7, the liquid-layer susceptibility $\bar{\chi}$ per solid-layer site is shown as a function of $\bar{n}$. This shows that $\bar{\chi}$ is at most of order of $(\gamma\hbar)^2\times(3 \text{ or } 4\ \mathrm{K}^{-1})$, which is 2 or 3 tenths of the solid-layer susceptibility at 20 mK. And, at $\bar{n}<0.7$, $\bar{\chi}$ is about 3% of the solid-layer susceptibility at 20 mK. Therefore the contributions from the liquid layers to the susceptibility are negligible at very low temperatures compared with that from the solid layer. This fact is also consistent with the experiments.[3),6)]

§ 4. Summary

We have reinvestigated the coverage dependence of the Curie-Weiss temperature T_c by taking all exchange constants into consideration and obtained the results which agree well with the experiment of Ref. 3). Also we have shown that the conclusions of I are unchanged: 1) The existence of the fourth layer is essential to make the system always ferromagnetic and 2) the decrease in T_c at higher coverage is caused by the increase in the effective mass of the liquid-layer atoms adjacent to the solid layer.

Also we have calculated the Curie constant and liquid-layer susceptibility, and found that 3) the Curie constant is almost independent of the liquid-layer density and that 4) the susceptibility of two liquid layers is negligible at low temperature compared with that of the solid layer.

Acknowledgements

The author would like to thank Professor T. Tsuneto for helpful discussions and continuous encouragement during the course of this work. He is also grateful to Dr. T. Ohmi for helpful discussions and useful comments.

Appendix A

After eliminating H_{l-s} to its first order, we have[4]

$$\bar{H}=H_s'+H_l'+V\,, \tag{A·1a}$$

where

$$V=\frac{1}{2}[S, H_{l-s}]+O\left(w\left(\frac{w}{\varepsilon_0}\right)^2\right), \tag{A·1b}$$

and H_s' and H_l' are the solid- and liquid-layer Hamiltonians including Zeeman terms, respectively. From Eq. (A·1), we will derive the effective Hamiltonian for the solid-layer atoms and Eqs. (3·5)~(3·6b) under the assumption that, when V is turned off, the ground and low-lying excited states $|\phi_\alpha\rangle$ of $\bar{H}$ tend to direct products of the eigenstates $|\chi_\alpha\rangle$ of H_s' and the ground state $|\zeta_B\rangle$ of H_l', i.e., $|\chi_\alpha\rangle|\zeta_B\rangle$.

The integral equation for $|\phi_\alpha\rangle$ in the Brillouin-Wigner perturbation theory is given by

$$\begin{aligned}|\phi_\alpha\rangle&=|\chi_\alpha\rangle|\zeta_B\rangle+\bar{P}_\alpha\frac{1}{E-H_s'-H_l'}V|\phi_\alpha\rangle\\&=|\chi_\alpha\rangle|\zeta_B\rangle+\bar{P}_\alpha\Omega|\phi_\alpha\rangle\,,\end{aligned} \tag{A·2a}$$

where

$$\Omega=i\int_0^\infty dt\; e^{-\eta t}\exp(i(H_s'+H_l')t)\,V\exp(-i\bar{H}t) \tag{A·2b}$$

and

$$\bar{P}_\alpha=1-|\chi_\alpha\rangle|\zeta_B\rangle\langle\zeta_B|\langle\chi_\alpha|\,. \tag{A·2c}$$

With the aid of $\bar{P}_\alpha'=1-|\chi_\alpha\rangle\langle\chi_\alpha|$ and $\bar{p}_B=1-|\zeta_B\rangle\langle\zeta_B|$, we can decompose Eq. (A·2a) into a couple of equations,

$$|\zeta_B\rangle\langle\zeta_B|\phi_\alpha\rangle=|\zeta_B\rangle|\chi_\alpha\rangle+|\zeta_B\rangle\bar{P}_\alpha'\langle\zeta_B|\Omega(|\zeta_B\rangle\langle\zeta_B|\phi_\alpha\rangle+\bar{p}_B|\phi_\alpha\rangle)\,, \tag{A·3a}$$

$$\bar{p}_B|\phi_\alpha\rangle=\bar{p}_B\Omega(|\zeta_B\rangle\langle\zeta_B|\phi_\alpha\rangle+\bar{p}_B|\phi_\alpha\rangle)\,. \tag{A·3b}$$

By solving Eq. (A·3b) with respect to $\bar{p}_B|\phi_\alpha\rangle$ and substituting the result into Eq. (A·3a), we get an equation for $|\phi_\alpha\rangle\leqq\langle\zeta_B|\phi_\alpha\rangle$,

$$|\phi_\alpha\rangle=|\chi_\alpha\rangle+\bar{P}_\alpha'\langle\zeta_B|\Omega(1-\bar{p}_B\Omega)^{-1}|\zeta_B\rangle|\phi_\alpha\rangle\,. \tag{A·4}$$

We define an effective interaction $V_{\rm eff}$ as a solution of the following equation:

$$i\int_0^\infty dt\; e^{-\eta t}\exp(iH_s't)\,V_{\rm eff}\exp(-i(H_s'+V_{\rm eff})t)=\langle\zeta_B|\Omega(1-\bar{p}_B\Omega)^{-1}|\zeta_B\rangle\,. \tag{A·5}$$

Then, by comparing Eq. (A·4) with Eq. (A·2a), we find that $|\phi_\alpha\rangle$ is an eigenstate of an effective Hamiltonian

$$H_s^{\rm eff}=H_s'+V_{\rm eff} \tag{A·6}$$

with an eigenvalue $\varepsilon_0'+\langle\chi_a|V_{\text{eff}}|\phi_a\rangle$, where ε_0' is the eigenvalue of H_s' corresponding to $|\chi_a\rangle$. From Eq. (A·3b), we also get

$$|\psi_a\rangle = W|\phi_a\rangle|\zeta_B\rangle\,, \tag{A·7}$$

where W is a mixing operator,

$$W=(1-\bar{p}_B\Omega)^{-1}\,. \tag{A·8}$$

Because the mixing operator W is not unitary, we need an extra constant C_N for normalization of $|\psi_a\rangle$,

$$C_N{}^2=\langle\zeta_B|\langle\phi_a|W^+W|\phi_a\rangle|\zeta_B\rangle/(\langle\phi_a|\phi_a\rangle\langle\zeta_B|\zeta_B\rangle)\,. \tag{A·9}$$

The effective interaction V_{eff} can be obtained perturbatively by expanding the left-hand side of Eq. (A·5) in V_{eff}.

Up to the second order in V, V_{eff} is given by

$$V_{\text{eff}}=\langle\zeta_B|V|\zeta_B\rangle+i\int_0^\infty dt\langle\zeta_B|V\bar{p}_BV(t)|\zeta_B\rangle e^{-\eta t}+O\left(w\left(\frac{w}{\varepsilon_0}\right)^3\right), \tag{A·10}$$

where

$$V(t)=\exp(i(H_s'+H_l')t)\,V\exp(-i(H_s'+H_l')t)\,.$$

This equation is Eq. (4·1a) of Ref. 4).*) And, up to the lowest order in V, C_N and W are given by Eqs. (3·6a) and (3·6b) respectively.

Appendix B

In this appendix, we show the ground-state properties of the liquid layers.

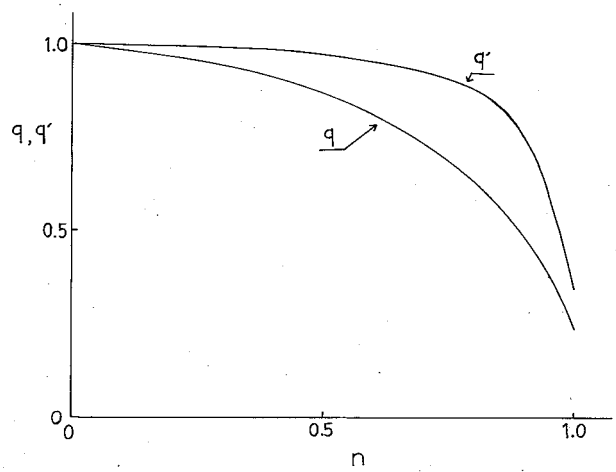

Fig. 8. The inverses of the mass enhancement factors for the third and fourth layers (q and q' respectively) vs the number $\bar{n}$ of liquid-layer atoms per site.

*) At first sight, the second term of Eq. (4·1a) of Ref. 4) seems to be different from that of Eq. (A·10). But this is not the case, as the term is real.

The liquid-layer ground state under zero magnetic field is well approximated by that of the effective Hamiltonian H_l^{eff} for the Kotliar-Ruckenstein auxiliary fermions $f_{i\sigma}$ and $f'_{i\sigma}$,[4),8)]

$$H_l^{\text{eff}}=L_2\sum_{i\sigma}f_{i\sigma}^{+}f_{i\sigma}-qT\sum_{(i,j)\sigma}f_{i\sigma}^{+}f_{j\sigma}+\sqrt{qq'}\sum_{k\sigma}w'(\boldsymbol{k})f_{k\sigma}^{+}f'_{k\sigma}+(\text{h.c.})$$
$$+(\varepsilon_1+L_2')\sum_{i\sigma}f_{i\sigma}'^{+}f'_{i\sigma}-q'T\sum_{(i,j)\sigma}f_{i\sigma}'^{+}f'_{j\sigma}\,. \qquad \text{(B·1)}$$

The inverses of the mass enhancement factors for the third- and fourth-layer atoms (q and q' respectively) and the molecular fields for the third- and fourth-layer atoms (L_2 and L_2' respectively) are determined, as well as the numbers of double occupations per site (D and D' respectively), by solving Eqs. (5·12a)~(5·12c′) of I.

In Fig. 8, q and q' are shown as functions of the number of the third-layer atoms per site n. The variable q starts appreciably deviating from 1.0 at $n\cong 0.5$, i.e., at $\bar{n}\cong 0.7$, which corresponds to the starting point of the appreciable decrease of T_c. Thus this also supports the interpretation that the increase of the effective mass of the third-layer atoms causes the decrease of T_c at higher coverage. The value of q' at

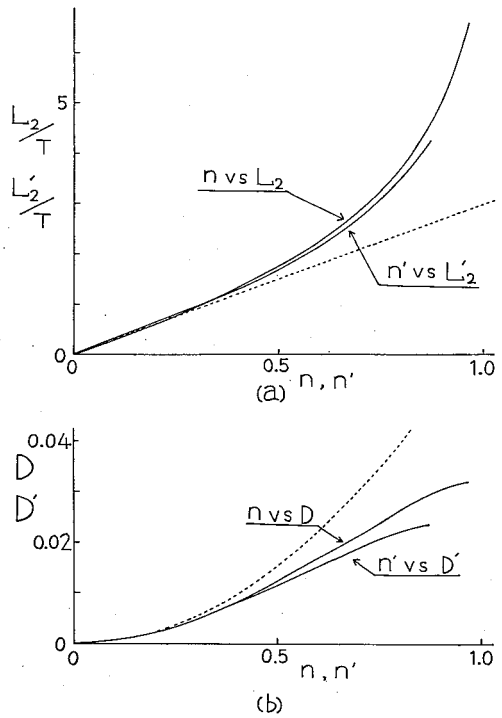

Fig. 9. (a) The molecular fields vs the numbers of atoms per site. Broken line shows a linear relation; $L_2=3Tn$.
(b) The numbers of double occupations per site vs the numbers of atoms per site. Broken line shows a Hartree-Fock-like behavior; $D=n^2/16$.

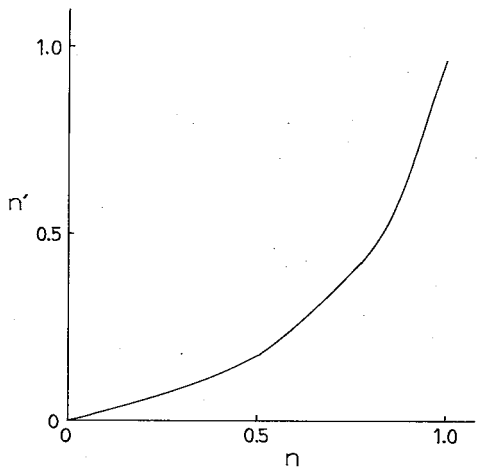

Fig. 10. The number of the third-layer atoms per site n vs that of the fourth-layer atoms n'.

$n=1$*) is 0.34, which agrees well with that of the bulk ^{3}He at zero pressure, i.e., 0.36.[9] And the value of q at $n=1$ is 0.24, which corresponds to that of the bulk liquid at 14 bar.[9]

In Fig. 9(a), L_2 and L_2' and, in Fig. 9(b), D and D' are shown as functions of n and n' respectively. At lower density, the system shows a Hartree-Fock-like behavior: The molecular fields L_2 and L_2' are linear in n and n' respectively and the numbers of double occupations per site D and D' are proportional to n^2 and n'^2 respectively. At higher density, the ^{3}He-^{3}He correlations become stronger and the numbers of double occupations are suppressed by the increase of the molecular fields.

In Fig. 10, we show the relation between the numbers of atoms per site in the third and fourth layers (n and n' respectively). At $n=0.6$, n' begins to increase rapidly. This is the reason why we approximate the fifth-layer formation by [4]

$$\rho_5/\rho_5^{\mathrm{com}}=\max(0,\, 2\rho_4/\rho_4^{\mathrm{com}}-1)\,,$$

where ρ_i denotes the areal density of the ith layer and ρ_i^{com} that of the completed ith layer. The value of n' at $n=1$ is 0.96. Since the density of the completed third layer is estimated as 0.072 atoms/Å^2,[4] that of the completed fourth layer is $0.072\times0.96=0.069$ atoms/Å^2, which corresponds to the bulk density of 0.028 mole/cm^3. This value agrees well with the density of liquid ^{3}He at the saturated vapor pressure,[10] i.e., 0.027 mole/cm^3.

The ground-state susceptibilities of the liquid layers are also calculated within the Kotliar-Ruckenstein formalism.[4),8] When $B\neq0$, the inverses of the mass enhancement factors and the molecular fields depend on spin values. When only the B-linear terms are retained, their self-consistent equations are reduced to linear equations for the third- and fourth-layer spin angular momenta per site (σ^z and σ'^z respectively) and the spin-antisymmetric parts of the third- and fourth-layer molecular fields (L_2^A and $L_2'^A$ respectively). Then the susceptibilities per site for the third and fourth layers (χ

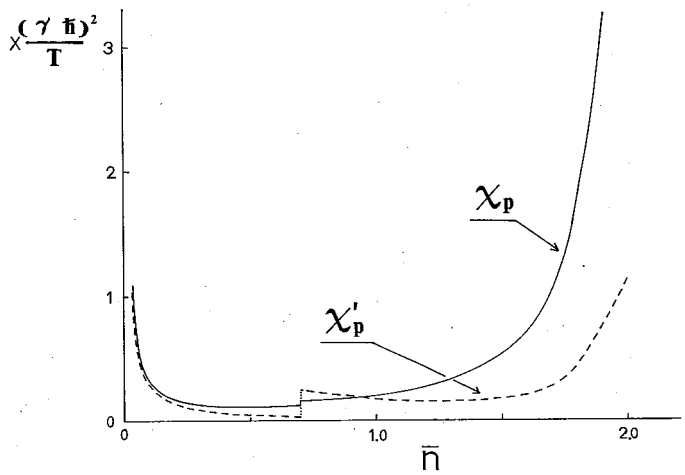

Fig. 11. Susceptibility per atom vs the number $\bar{n}$ of liquid-layer atoms per site. χ_p for the third layer and χ_p' for the fourth layer.

*) All these calculations are carried out numerically. Since, at $n=1$, the convergence is very bad, we obtain the physical quantities at $n=1$ by extrapolating those at $n=0.96$ and at $n=0.97$.

and χ' respectively) are given by $\chi=\sigma^z/B$ and $\chi'=\sigma'^z/B$. Note that the liquid-layer susceptibility per solid-layer site $\bar{\chi}$, of which coverage dependence has been shown in § 3, is given by $\bar{\chi}=(a'/a)^2(\chi+\chi')$.

In Fig. 11, the susceptibilities per atom $\chi_P=\chi/n$ and $\chi_P'=\chi'/n'$, respectively, for the third and fourth layers are shown as functions of $\bar{n}$. As before, the finiteness of the band-edge density of states of the upper band causes the discontinuity at $\bar{n}\cong 0.7$. The rapid decrease at $\bar{n}\leqq 0.15$ indicates the crossover from the free spin system (which obeys Curie law) to the degenerate Fermi gas. The figure shows that the liquid layers at $\bar{n}=0.56$ are well degenerate, which agrees with the result of Ref. 6). At $\bar{n}\leqq 0.15$, the liquid layers lose the properties of degenerate Fermi gas and the indirect spin exchange induced by them must be disturbed by the effect of temperature. This provides another reason why the peak of the Curie-Weiss temperature at $\bar{n}\cong 0$, which is predicted in § 2, is not observed. Finally, the increase of χ_P and χ_P' at $\bar{n}\geqq 1.5$ shows the crossover from the ordinary to almost-localized Fermi gas.

References

1) A. I. Ahonen, T. Kodama, M. Krusius, M. A. Paalanen, R. C. Richardson, W. Schoepe and Y. Takano, J. of Phys. **C9** (1976), 1665.
A. I. Ahonen, T. A. Alvesalo, T. Haavasoja and M. C. Veuro, Phys. Rev. Lett. **41** (1978), 494.
H. Godfrin, G. Frossati, D. Toulouze, M. Chappellier and W. G. Clark, J. Phys. Colloque **39** (1978), C6-287.
H. M. Bozler, T. Bartolac, K. Luey and A. L. Thomson, Phys. Rev. Lett. **41** (1978), 490.
Y. Okuda, A. J. Ikushima and H. Kojima, Phys. Rev. Lett. **54** (1985), 130.
Y. Okuda and A. J. Ikushima, Phys. Rev. **B33** (1986), 3560.
2) M. T. Béal-Monod and S. Doniach, J. Low Temp. Phys. **28** (1977), 175.
R. A. Guyer, Phys. Rev. Lett. **39** (1977), 1091.
D. Spaniaard, D. L. Mills and M. T. Béal-Monod, J. Low Temp. Phys. **34** (1979), 307.
J. M. Delrieu, M. Roger and J. H. Hetherington, J. Low Temp. Phys. **40** (1980), 71.
H. Jichu and Y. Kuroda, Prog. Theor. Phys. **67** (1982), 715; **69** (1983), 1358.
M. Roger, Phys. Rev. **B30** (1984), 6432.
M. Roger and J. M. Delrieu, Jpn. J. Appl. Phys. Suppl. **26-3** (1987), 267.
3) H. Franco, R. E. Rapp and H. Godfrin, Phys. Rev. Lett. **57** (1986), 1161.
4) S. Tasaki, Prog. Theor. Phys. **79** (1988), 1311; **80** (1988), 922E.
5) N. Sullivan, G. Deville and A. Landesman, Phys. Rev. **B11** (1975), 1858.
6) H. Godfrin, R. R. Ruel and D. D. Osheroff, Phys. Rev. Lett. **60** (1988), 305.
7) J. R. Schrieffer and P. A. Wolff, Phys. Rev. **149** (1966), 491.
8) G. Kotliar and A. E. Ruckenstein, Phys. Rev. Lett. **57** (1986), 1362.
9) D. Vollhardt, Rev. Mod. Phys. **56** (1984), 99.
10) D. F. Brewer, in *Physics of Liquid and Solid Helium*, ed. K. H. Bennemann and J. B. Ketterson (Wiley, New York, 1978), Part 2.